Age of host rocks at the Chianti Cu-Au Prospect, eastern Gawler Craton from zircon U-Pb geochronology

Anthony Reid and Adrian Fabris

Government of South Australia

Department for Manufacturing, Innovation, Trade, Resources and Energy

Report Book
2012/00014

Age of host rocks at the Chianti Cu-Au Prospect, eastern Gawler Craton from zircon U-Pb geochronology

Anthony Reid, Adrian Fabris

**Geological Survey of South Australia,
Resources and Energy Group, DMITRE**

October 2012

Report Book 2012/00014

Government of South Australia
Department for Manufacturing,
Innovation, Trade, Resources and Energy

Resources and Energy Group
Department for Manufacturing, Innovation, Trade, Resources and Energy
Level 7, 101 Grenfell Street, Adelaide
GPO Box 1264, Adelaide SA 5001
Phone +61 8 8463 3037
Email dmitre.minerals@sa.gov.au
www.minerals.dmitre.sa.gov.au

South Australian Resources Information Geoserver (SARIG)
SARIG provides up-to-date views of mineral, petroleum and geothermal tenements and other geoscientific data. You can search, view and download information relating to minerals and mining in South Australia including tenement details, mines and mineral deposits, geological and geophysical data, publications and reports (including company reports).
www.sarig.dmitre.sa.gov.au

Preferred way to cite this publication
Reid A and Fabris A 2012. *Age of host rocks at the Chianti Prospect Cu-Au, eastern Gawler Craton from zircon U-Pb geochronology*, Report Book 2012/00014. Department for Manufacturing, Innovation, Trade, Resources and Energy, South Australia, Adelaide.

CONTENTS

TABLES

FIGURES

Age of host rocks at the Chianti Prospect Cu-Au, eastern Gawler Craton from zircon U-Pb geochronology

Anthony Reid, Adrian Fabris

INTRODUCTION

The primary aim of the U-Pb geochronology presented here was to constrain the age of granites that form the principal host unit to the minor mineralisation and extensive alteration present within the Chianti Cu-Au prospect, eastern Gawler Craton (Fig. 1; Paterson, 2007). A sample of the sedimentary unit that is present within one drill hole was also examined to see if there could be a relationship between these sediments and those recently described from the Olympic Dam deposit (McPhie et al., 2011).

A particular difficulty with this geochronology program was the highly metamict and altered nature of many of the zircons separated from the samples. In particular, the zircons from the sedimentary rock were very poor quality, which meant that the amount and quality of the U-Pb data collected from these samples was limited. Therefore the data presented here from a number of the samples should be regarded as reconnaissance in nature. Further work with different samples may be required to fully characterize the geochronology of this prospect.

CHIANTI PROSPECT

The Chianti Prospect is a residual gravity anomaly located approximately 98 km to the south-southeast of Olympic Dam, occurring within the Olympic Cu-Au Province of the eastern Gawler Craton (Fig. 1; Paterson, 2007). Several diamond drill holes at this prospect have intersected sericite-chlorite-hematite ± carbonate altered granitiods, volcanics and clastic sediments together with narrow zones of Cu-Au mineralisation within intensely hematite altered and brecciated rock at depths of between 400 and 600m below surface. The best intercept from this prospect was from drillhole DDH MGD34, which had visible chalcopyrite and bornite within quartz-rich hematite veining and gave 2.01% Cu, 0.10 ppm Au, 2.4 ppm Ag, over the depth interval 548-552m (Paterson, 2007).

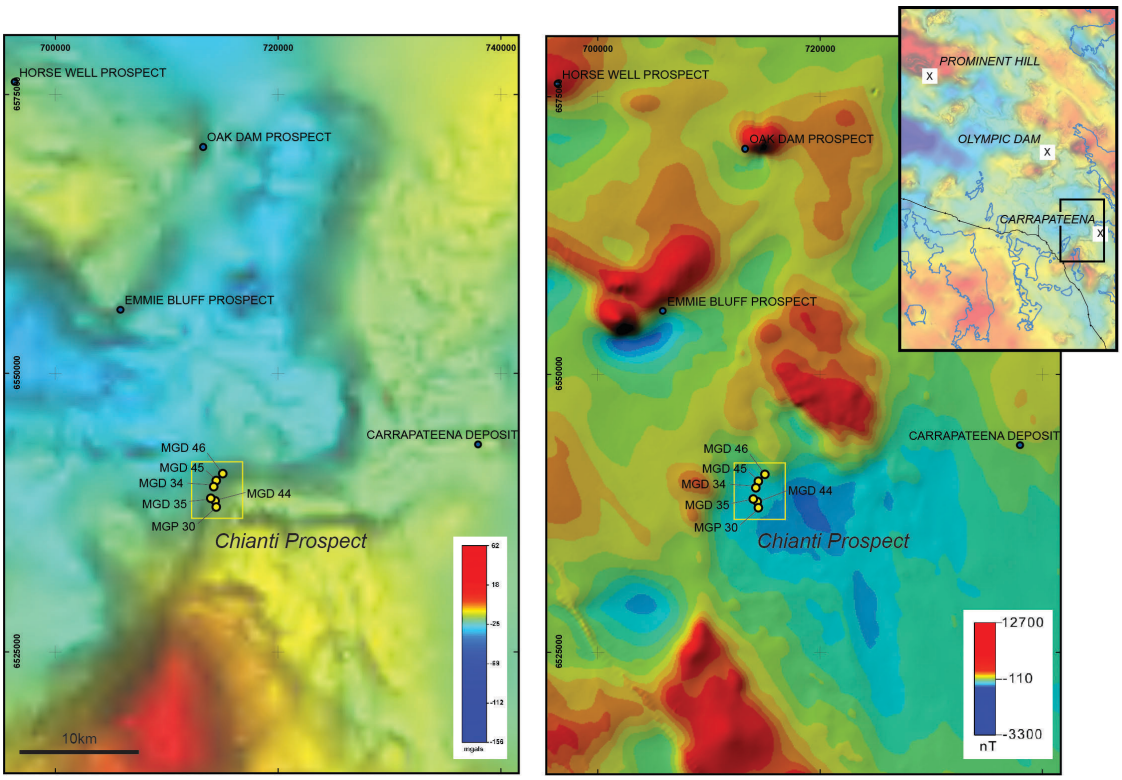

Figure 1. Location of the Chianti pProspect and basement intersecting drillholes from within the prospect area. Drillholes sampled as part of this study include MGD44, 45, 46. Left is a regional bouguer gravity image. Right is total magnetic intensity image. Inset shows location of the image with respect to the regional gravity data and the location of Olympic Dam, Prominent Hill and Carrapateena.

Table 1. Summary of samples analysed in this study.

Sample	Drillhole, depth	Rock type	Method	Interpreted age	Age type	n/total analyses
1831650	DDH MGD45, 738.10–738.80 m	monzogranite	LA-ICPMS	1848 ± 15 Ma	Magmatic crystallisation	7/14
1831646	DDH MGD45, 667.05–667.30 m	monzogranite	LA-ICPMS	1857 ± 19 Ma	Magmatic crystallisation	5/10
1831656	DDH MGD46, 705.10–706.00 m	medium-grained granite	LA-ICPMS	1844 ± 22 Ma	Magmatic crystallisation	4/4
1848980	DDH MGD44, 425.60–426.00 m	volcaniclastic sediment	LA-ICPMS	n/a		
1842343	DDH MGD44, 511.30–511.70 m	granite	LA-ICPMS	1858 ± 22 Ma	Magmatic crystallisation	9/19
1901138	DDH MGD44, 326.15–327.90 m	microgranite	SHRIMP	1591 ± 10 Ma	Magmatic crystallisation	6/13

GEOCHRONOLOGICAL METHODS

LA-ICPMS METHODS

Rock samples were scrubbed, washed, dried then crushed at a commercial mineral separation facility, MinSep Labs, Denmark, Western Australia (www.minsep.com), following which standard density and magnetic separation techniques were used to isolate zircon crystals from the crushed rock. Zircons were then mounted in epoxy disc and polished so as to expose the grains at the surface.

This study utilised a 213 nm New Wave Research laser ablation unit coupled with an Agilent 7300 quadrupole ICPMS different at Adelaide Microscopy, the University of Adelaide, with methods identical to those reported previously (Payne et al., 2006; Reid et al., 2006). The 213 nm laser unit was run using a 30 μm spot size and a 5 Hz repetition rate. Analytical spot size was 30 μm. Time-resolved signals of $^{204, 206, 207, 208}$Pb, ^{232}Th and ^{238}U were acquired during a 90 second analytical interval, comprising 40 seconds of analysis of the background signal, before the onset of laser ablation and the subsequent collection of 50 seconds worth of analytical signal related to the sample being analysed. The LA-ICPMS process causes elemental and isotopic fractionation as a result of the nature of the laser ablation process and during ionisation of the ablated material within the plasma. To correct for this instrument-induced fractionation, unknown zircons are analysed along with a well characterized standard zircon, GJ-1, which has a similar crystal matrix and hence results in similar fractionation profiles during the analysis. This matrix matching process enables correction for fractionation by bracketing the unknown with known analyses (Belousova et al., 2001; Jackson et al., 2004). In addition to the GJ-1 zircon as an internal standard, each session also included analysis of 'external' standards; zircons of known age as checks on instrument performance. In this study we have used the standard zircons QGNG (1851.6 ± 1.0 Ma; Black et al., 2003) and Plešovice (337.13 ± 0.37 Ma; Sláma et al., 2007). Data from the ICPMS were processed using the GLITTER software to select intervals over which the analytical signal is integrated to produce the isotopic ratios and ages for individual zircons analyses (Griffin et al., 2008). Weighted mean ages and concordia diagrams were constructed using Isoplot 3 (Ludwig, 2003).

SHRIMP GEOCHRONOLOGY METHODS

Zircon U-Pb geochronology was also undertaken via sensitive high resolution ion microprobe (SHRIMP) analysis at the John De Laeter Centre for Mass Spectrometry, Curtin University, Perth. Zircons were extracted from the rock samples through standard crushing, density, magnetic separation procedures. Zircon grains were encapsulated in epoxy, together with the multi-grain zircon standards OG1 (^{207}Pb/^{206}Pb standard) and Temora 2 (U-Pb standard). A small quantity of the zircon standard BR266 (903 ppm U) was used as a U concentration standard. The mount was polished to expose grains in section. All grains were photographed in transmitted and reflected light, and imaged by cathodoluminescence (CL).

Isotopic data were collected using a primary oxygen ion beam of ~1.7–2.5 nA intensity and ~20 microns diameter using the SHRMIP A instrument. Differential fractionation between U and Pb was monitored by reference to a ^{206}Pb/^{238}U ratio of 0.0668 for interspersed analyses of the 416.8 ± 0.3 Ma Temora 2 zircon standard (Black et al., 2003), based on the power law relationship $^{206}Pb^{+}/U^{+} = a(UO^{+}/U^{+})^{2}$. Th/U ratios were derived from the linear relationship ^{232}ThO/^{238}U = (0.03446.UO+/U++0.868). ThO+/UO+. Temora 2 was also used to monitor isobaric interference at the ^{204}Pb mass peak. The 3465.4 ± 0.6 Ma OG1 standard (Stern et al., 2009) was used to monitor ^{207}Pb/^{206}Pb reproducibility and accuracy. Radiogenic Pb compositions were initially determined by subtracting contemporaneous common Pb (Stacey and Kramers, 1975). Data were processed using SQUID 2 (Ludwig, 2009) and plotted using ISOPLOT/EX 3.71 (Ludwig, 2003), using the U and Th decay constants of Jaffey et al. (1971), as recommended by Steiger and Jäger (1977). Uncertainties are quoted at the 95% (tσ) confidence level.

LA-ICPMS RESULTS

1831650, ALTERED GRANITE, DDH MGD45, CHIANTI PROSPECT

Sample information

Sample Number:	1831650		
Collector:	A Reid		
Stratigraphic Unit:			
Location GDA94:	714464	6540377	Zone 53
Location Lat-Long:	-31.2511444	137.2521487	
250K map sheet	SH5316 TORRENS		
100K map sheet	6335 ARCOONA		
Location:	DDH MGD45, 738.10 - 738.80m		
Mount:	AR-15		
Date analysed:	19th May 2011		
Machine:	New Wave LA-ICPMS Adelaide Microscopy		
Concurrent Standard data	QGNG standard: 1846 ± 20 (n = 4, MSWD = 0.065, probability = 0.98) Plešovice standard: 331.1 ± 4.5 Ma (n = 4, MSWD = 0.92, probability = 0.43)		
Interpreted age:	1848 ± 15 Ma		
Age type:	Magmatic crystallisation		
Age calculation method	weighted mean $^{207}Pb/^{206}Pb$ age		

Background

This sample is an altered coarse-grained granite (Fig 2) that represents the dominant granitic lithology in the MGD series of drillholes.

Figure 2. Photograph of rock sample 1831650.

Petrography

Sample 1831650 is an altered coarse-grained monzogranite. The sample contains large crystals of quartz that together with the feldspar form a granoblastic texture (Fig. 3). Quartz shows no undulose extinction suggesting this rock has experienced little strain. Feldspar within this sample is extensively altered to mats of sericite plus hematite, the patchiness of the altered feldspars gives the sample its characteristic blotchy red texture in hand specimen. The feldspars include plagioclase and K-feldspar, with the former being approximately An60, labrodorite in composition. K-feldspar is present as sericite altered crystals. Biotite is approximately 5% of the sample. No primary igneous muscovite is observed. Moderately coarse grained sericite is present in the centres of some of the larger plagioclase crystals. Biotite is extensively replaced by chlorite plus hematite. Zircon is present as a trace mineral, often occurring along grain boundaries between biotite and quartz, or quartz and plagioclase.

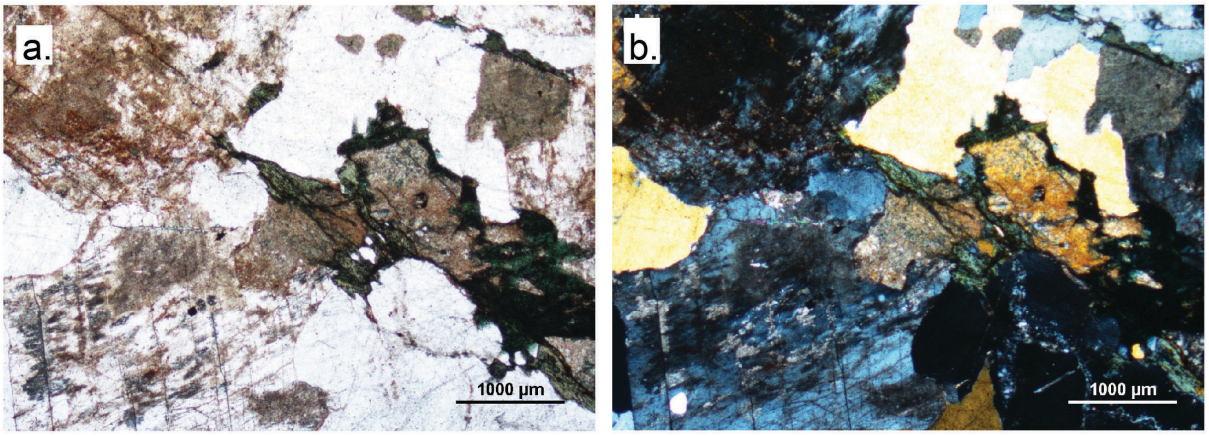

Figure 3. Photomicrographs of sample 1831650. a. Transmitted plain polarised light. **b.** Cross polars.

Zircon characteristics

Zircons from this sample are mostly subhedral in morphology, with low length to width ratios. Many of the grains are transparent, although many of the larger grains are very dark and cracked (Fig. 4). Under CL the grains show internal zones of light CL response, many of which have oscillatory zonation. The outer portion of many of the grains, however comprises a rim characterised by dark CL response, indicative of high U contents. There are also some grains that have dark CL zones that occur within the light CL zones, or that transgress the light CL regions.

Geochronological results

Fourteen analyses were collected on zircons from sample 1831650 (Table 2). Nine of these data points are near concordant, with the remaining being discordant, some extremely so. The majority of data from the light CL domains return $^{207}Pb/^{206}Pb$ ages that cluster at c. 1850 Ma (Fig. 5). A weighted mean $^{207}Pb/^{206}Pb$ age calculated from seven of the concordant to near concordant data is 1848 ± 15 Ma (MSWD = 0.92, probability = 0.48). Analysis of the high U zones produced very discordant data, all of which plot towards non-radiogenic compositions on the Tera-Wasserburg diagram, indicating these regions that have been analysed are high in common Pb. Consequently, the ages derived from these analyses are unreliable.

Geochronological interpretation

The weighted mean $^{207}Pb/^{206}Pb$ age of 1848 ± 15 Ma is interpreted to be the timing of emplacement of the granodiorite. The timing of the dark CL, high U, regions from the zircons of this sample is not constrained.

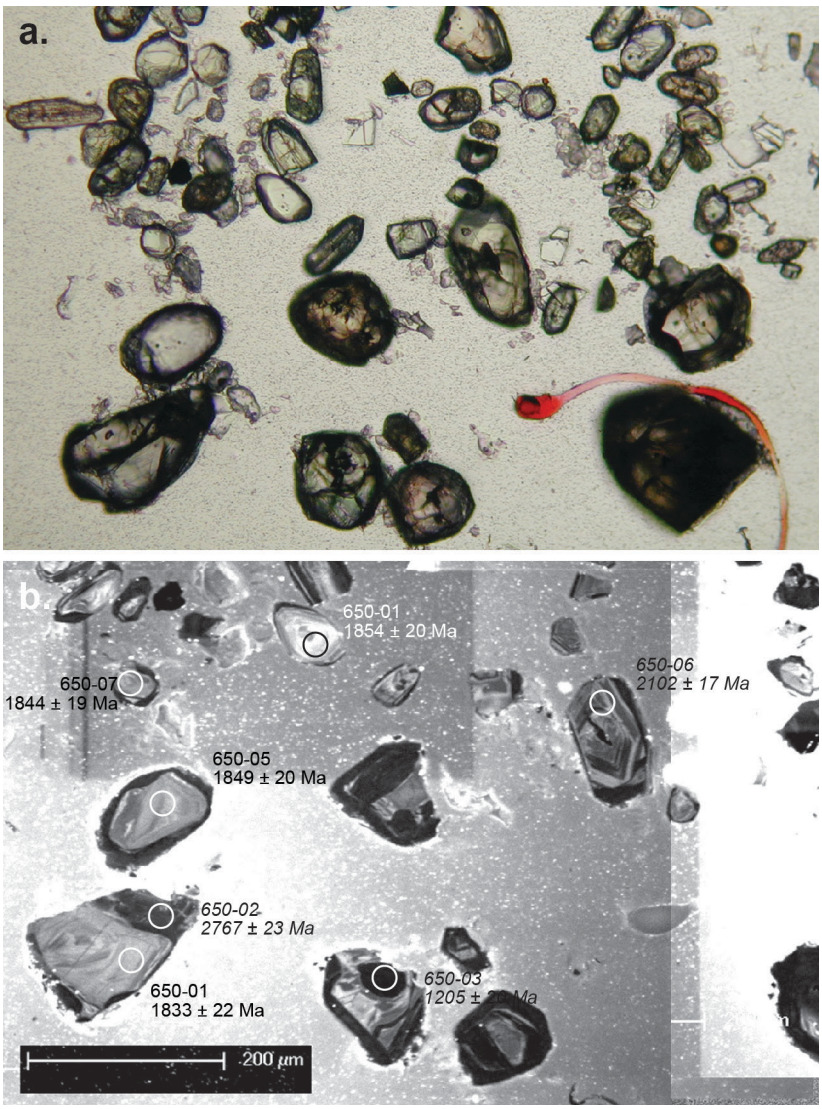

Figure 4. Representative zircons from sample 1831650. a. Plain light image. **b.** CL image. Circles indicate analytical site. Italics in the numbers indicates data is >10% discordant.

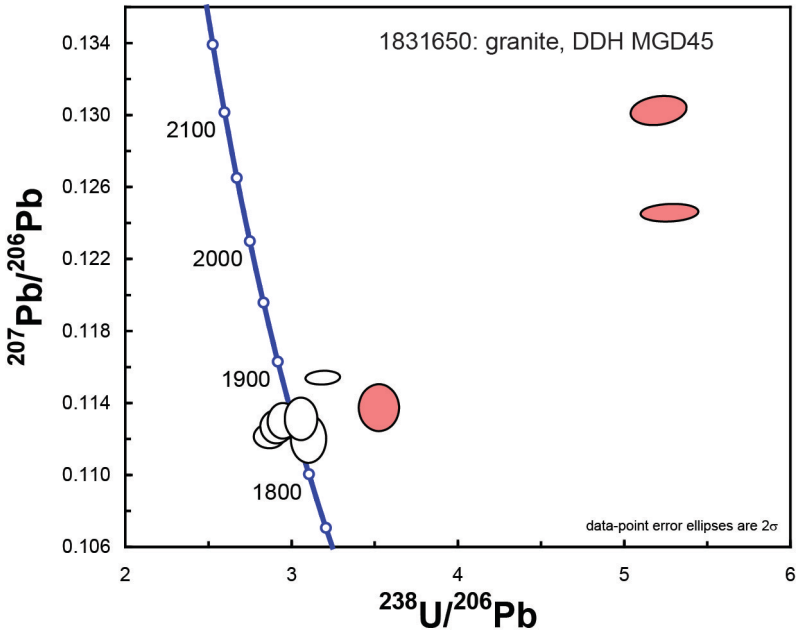

Figure 5. Concordia diagram for sample 1831650. White ellipses indicate those analyses included in the weighted mean age calculation. Analyses 650-2 and 650-3 not shown.

Table 2. Summary of LA-ICPMS data for sample 1831650.

Analysis	Isotopic ratio						Age				
	Pb^{207}/Pb^{206}	1σ	Pb^{206}/U^{238}	1σ	Pb^{207}/U^{235}	1σ	Pb^{207}/Pb^{206}	1σ	Pb^{206}/U^{238}	1σ	% Disc.
650-1	0.1121	0.0014	0.322	0.005	4.975	0.075	1833	22	1800	22	2
650-2	0.1930	0.0019	0.093	0.001	2.475	0.032	2767	16	573	7	79
650-3	0.0803	0.0008	0.020	0.000	0.219	0.003	1205	20	126	2	90
650-5	0.1130	0.0013	0.339	0.004	5.282	0.070	1849	20	1882	21	-2
650-4	0.1131	0.0013	0.327	0.004	5.095	0.069	1850	21	1822	21	2
650-6	0.1303	0.0013	0.192	0.003	3.448	0.045	2102	17	1132	14	46
650-7	0.1127	0.0012	0.331	0.005	5.145	0.071	1844	19	1843	22	0
650-8	0.1246	0.0013	0.190	0.003	3.256	0.043	2023	18	1119	14	45
650-9	0.1128	0.0012	0.337	0.005	5.242	0.074	1846	20	1872	22	-1
650-10	0.1128	0.0012	0.329	0.004	5.117	0.070	1844	19	1834	22	1
650-11	0.1154	0.0012	0.313	0.004	4.984	0.066	1887	18	1756	20	7
650-12	0.1122	0.0012	0.348	0.005	5.387	0.073	1835	19	1926	22	-5
650-13	0.1139	0.0014	0.283	0.004	4.445	0.066	1862	22	1608	20	14
650-14	0.1127	0.0013	0.343	0.005	5.334	0.076	1843	20	1902	23	-3

1831646, MONZOGRANITE, DDH MGD45, CHIANTI PROSPECT

Sample information

Sample Number:	1831646		
Collector:	A Reid		
Stratigraphic Unit:	Donington Suite		
Location GDA94:	714464	6540377	Zone 53
Location Lat-Long:	-31.2511444	137.2521487	
250K map sheet	SH5316 TORRENS		
100K map sheet	6335 ARCOONA		
Location:	DDH MGD45, 667.05 - 667.30m		
Mount:	AR-15		
Date analysed:	18th May 2011		
Machine:	New Wave LA-ICPMS Adelaide Microscopy		
Concurrent Standard data	QGNG standard: 1846 ± 20 (n = 4, MSWD = 0.065, probability = 0.98) Plešovice standard: 331.1 ± 4.5 Ma (n = 4, MSWD = 0.92, probability = 0.43)		
Interpreted age:	1857 ± 19 Ma		
Age type:	Magmatic crystallisation		
Age calculation method	weighted mean $^{207}Pb/^{206}Pb$ age		

Background

This sample is a pink-coloured granitic dyke that intrudes the coarse grained granite within this drill hole (Fig. 6).

Figure 6. Image of core from Hylogger scan of DDH MGD45, showing the pink granitic dyke that intrudes the grey coloured altered coarse-grained granite.

Petrography

Sample 1831646 is an altered coarse-grained monzogranite. The sample contains large crystals of quartz that show weak or no undulose extinction suggesting this rock has experienced little strain (Fig. 7). Both plagioclase and K-feldspar are present within the sample. The plagioclase is An68, labrodorite in composition and is extensively altered to a fine mat of sericite and hematite. K-feldspar shows cross hatch twinning. The granite possesses only minor biotite, which occurs as large crystals <2 mm long. The biotite is extensively replaced by chlorite plus hematite. Very minor muscovite is also present as elongate laths to 1mm in length, occurring adjacent to altered biotite. Both biotite and muscovite are primary igneous minerals. The hematite-dusting evident within the plagioclase imparts a distinct red appearance to the hand specimen.

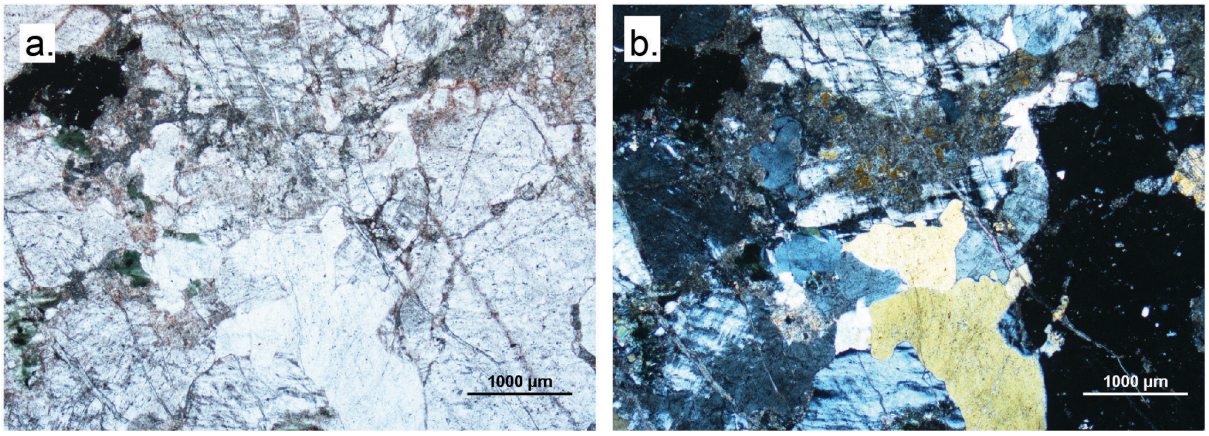

Figure 7. Photomicrographs of sample 1831646. a. Transmitted plain polarised light. **b.** Cross polars.

Zircon characteristics

Zircons from this sample are generally subheral to euhedral grains with low length to width ratio. The grains are brown to light brown in colour and are variably cracked (Fig. 8). The CL image reveals the grains to be composed of oscillatory zoned cores overgrown by very dark, high U rims (Fig. 8). In some examples these 'rims' appear to transgress the oscillatory zoned zircon domains suggesting this phase of zircon growth occurred either during a second phase of magmatism or due to the influx of hydrothermal fluids.

Geochronological results

Ten analyses were collected on zircons from sample 1831646 (Table 3; Fig. 9) These data are mostly discordant; except four analyses, all are >10% discordant. The discordant data points plot towards non-radiogenic Pb compositions on a Tera-Wasserburg concordia diagram, indicating these zircons are likely rich in non-radiogenic Pb accounting for their much older $^{207}Pb/^{206}Pb$ ages compared with the concordant data points. The concordant data points all derive from analyses of light CL oscillatory zoned zircon. A weighted mean $^{207}Pb/^{206}Pb$ age calculated from the near concordant data points is 1857 ± 19 Ma (n = 5; MSWD = 0.13, probability = 0.97), which omits the analyses 646-3, -5, -7, -8 and -10. This is identical to a concordia upper intercept age of 1854.4 ± 9.4 Ma which can be calculated using the same data points. The lower intercept of this discordia is within uncertainty of zero suggesting the minor Pb loss is recent.

Analysis 10 is from a large portion of black zircon on the rim of a light CL oscillatory zoned core. These data are strongly discordant and do not provide any constraint on the timing of crystallisation of these rims. If these rims represent a magmatic phase of zircon growth, the c. 1857 Ma age from the cores is only a maximum age for the timing of crystallisation of the pegmatite. It may have been emplaced younger than this, if the oscillatory zoned cores are inherited grains within a low temperature melt. Alternatively, the dark CL rims may be a late stage magmatic fluid, in which case 1857 ± 19 Ma may in fact be the age of emplacement of this pegmatite.

Geochronological interpretation

The weighted mean $^{207}Pb/^{206}Pb$ age of 1857 ± 19 Ma provides the maximum constraint on the timing of emplacement of this pegmatite. However, the inability to date the dark, high U rims means that the actual timing of emplacement is uncertain.

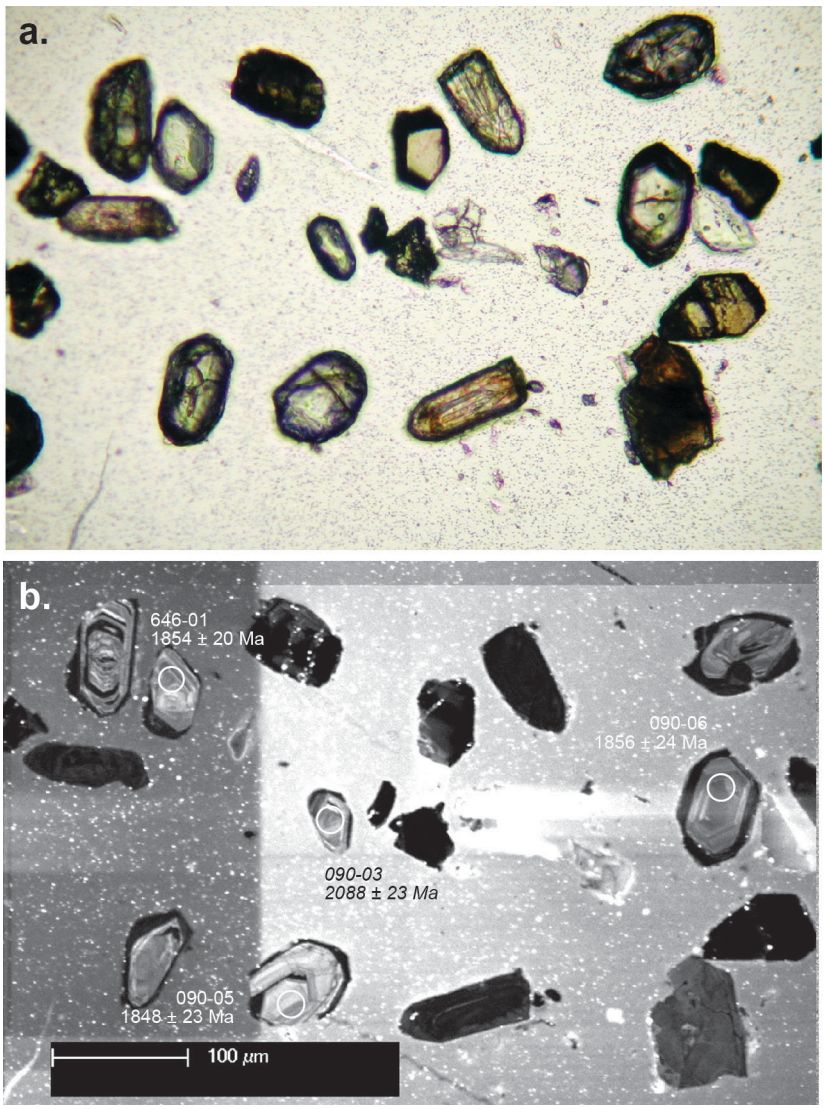

Figure 8. Representative zircons from sample 1831646. a. Plain light image. **b.** CL image. Circles indicate analytical site. Italics in the numbers indicates data is >10% discordant.

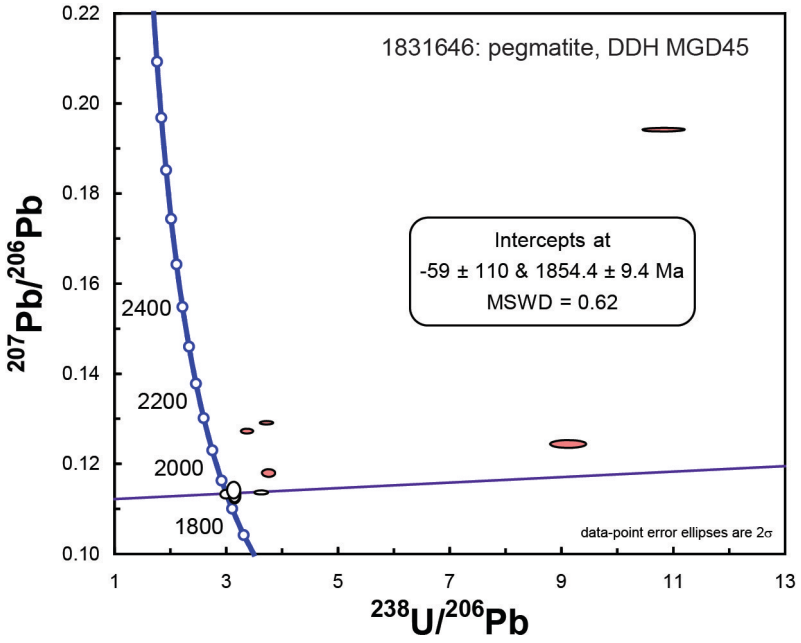

Figure 9. Concordia diagram for sample 1831646. White ellipses indicate those analyses included in the weighted mean age calculation.

Table 3. Summary of LA-ICPMS data for sample 1831646.

Analysis	Isotopic ratio						Age				
	Pb^{207}/Pb^{206}	1σ	Pb^{206}/U^{238}	1σ	Pb^{207}/U^{235}	1σ	Pb^{207}/Pb^{206}	1σ	Pb^{206}/U^{238}	1σ	% Disc.
646-1	0.1134	0.0013	0.335	0.004	5.234	0.071	1854	20	1862	21	0
646-2	0.1130	0.0014	0.318	0.004	4.954	0.075	1848	23	1781	22	4
646-3	0.1292	0.0013	0.269	0.004	4.797	0.064	2088	18	1537	18	26
646-4	0.1135	0.0015	0.319	0.004	4.984	0.075	1856	24	1783	21	4
646-5	0.1181	0.0013	0.267	0.004	4.339	0.060	1927	19	1523	18	21
646-6	0.1144	0.0015	0.320	0.005	5.045	0.082	1870	24	1790	23	4
646-7	0.1246	0.0014	0.110	0.002	1.883	0.028	2023	20	671	9	67
646-8	0.1274	0.0013	0.297	0.004	5.218	0.071	2063	18	1677	20	19
646-9	0.1138	0.0012	0.276	0.004	4.334	0.061	1861	19	1573	20	15
646-10	0.1943	0.0020	0.092	0.001	2.475	0.035	2779	17	570	8	80

1831656, MEDIUM GRAINED GRANITE, DDH MGD46, CHIANTI PROSPECT

Sample information

Sample Number:	1831656		
Collector:	A Reid		
Stratigraphic Unit:	Donington Suite		
Location GDA94:	715052	6540987	Zone 53
Location Lat-Long:	-31.245536	137.258188	
250K map sheet	SH5316 TORRENS		
100K map sheet	6335 ARCOONA		
Location:	DDH MGD46, 705.10–706.00 m		
Mount:	AR-15		
Date analysed:	18th May 2011		
Machine:	New Wave LA-ICPMS Adelaide Microscopy		
Concurrent Standard data	QGNG standard: 1846 ± 20 (n = 4, MSWD = 0.065, probability = 0.98) Plešovice standard: 331.1 ± 4.5 Ma (n = 4, MSWD = 0.92, probability = 0.43)		
Interpreted age:	1844 ± 22 Ma		
Age type:	Magmatic crystallisation		
Age calculation method	weighted mean $^{207}Pb/^{206}Pb$ age		

Background

This sample is an altered granite representative of the altered granite within drill hole MGD 46.

Petrography

Sample 1831656 is a medium-grained granite, comprising quartz, plagioclase, K-feldspar, biotite and muscovite. The quartz shows abundant undulose extinction and in places shows subgrain development, consistent with the sample having undergone some degree of strain (Fig. 10). The feldspars are extensively replaced by microcrystalline intergrowth of sericite plus hematite. The sample shows a distinctive pattern in alteration of the feldspars. Plagioclase is more pervasively retrogressed to fine sericite plus hematite, while relict primary igneous twinning is more readily observed within the K-feldspar (microcline). Muscovite is the dominant mica phase within the sample, occurring as elongate laths up to 4mm in length within the granoblastic texture. Biotite is less common, present as smaller laths of dark brown coloured igneous crystals. Dissecting the rock are hematite plus chlorite filled fractures. Hematite plus chlorite also infiltrate along grain boundaries forming a network of alteration within the rock. Within some of the fractures are small laths of muscovite (sericite). Pleochronic brown, anhedral biotite is also present, associated with the chlorite+hematite alteration. In places small apatite crystals are also observed and are associated with the chlorite-rich alteration.

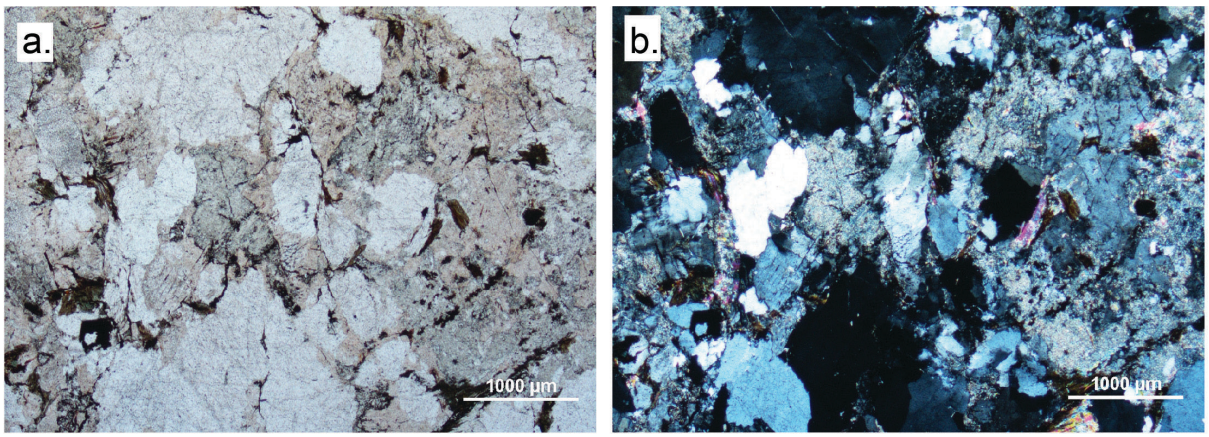

Figure 10. Photomicrographs of sample 1831656. a. Transmitted plain polarised light. **b.** Cross polars.

Zircon characteristics

Very few zircons were recovered from this sample. The majority of grains within the mineral separate appear to be apatite. Those grains that are zircon are generally transparent, with low length to width ratios (Fig. 11). The CL image reveals a similar pattern to the two previous samples in that there is an internal zone of light oscillatory zoned zircon that is mantled by a dark CL phase.

Geochronological results

Because of the low zircon yield, only four grains were analysed from this sample (Table 4; Fig. 12). All analyses were from zones of light CL response, and thus most likely from magmatic zircon. The data are all within ±10% of Concordia and have $^{207}Pb/^{206}Pb$ ages that cluster at c. 1850 Ma. A weighted mean $^{207}Pb/^{206}Pb$ age calculated the four analyses 1844 ± 22 Ma (MSWD = 0.27, probability = 0.85).

Geochronological interpretation

The weighted mean $^{207}Pb/^{206}Pb$ age of 1844 ± 22 Ma is interpreted to be the timing of emplacement of the granodiorite. The timing of the dark CL, high U, regions from the zircons of this sample is not constrained.

Table 4. Summary of LA-ICPMS data for sample 1831656.

Analysis	Isotopic ratio						Age				
	Pb^{207}/Pb^{206}	1σ	Pb^{206}/U^{238}	1σ	Pb^{207}/U^{235}	1σ	Pb^{207}/Pb^{206}	1σ	Pb^{206}/U^{238}	1σ	% Disc.
656-1	0.1130	0.0026	0.334	0.005	5.201	0.117	1848	40	1857	25	-1
656-2	0.1118	0.0013	0.339	0.004	5.228	0.074	1828	22	1883	22	-3
656-3	0.1134	0.0013	0.337	0.005	5.270	0.074	1854	20	1873	22	-1
656-4	0.1129	0.0012	0.335	0.005	5.211	0.071	1846	19	1862	22	-1

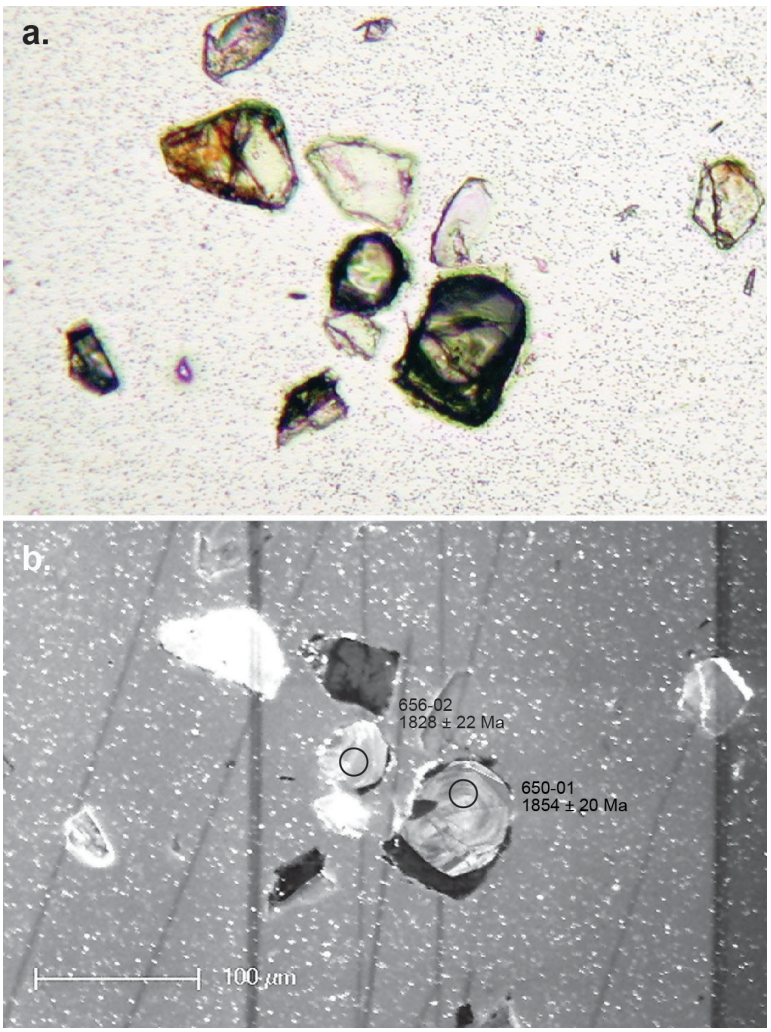

Figure 11. Representative zircons from sample 1831656. a. Plain light image. **b.** CL image. Circles indicate analytical site. Italics in the numbers indicates data is >10% discordant.

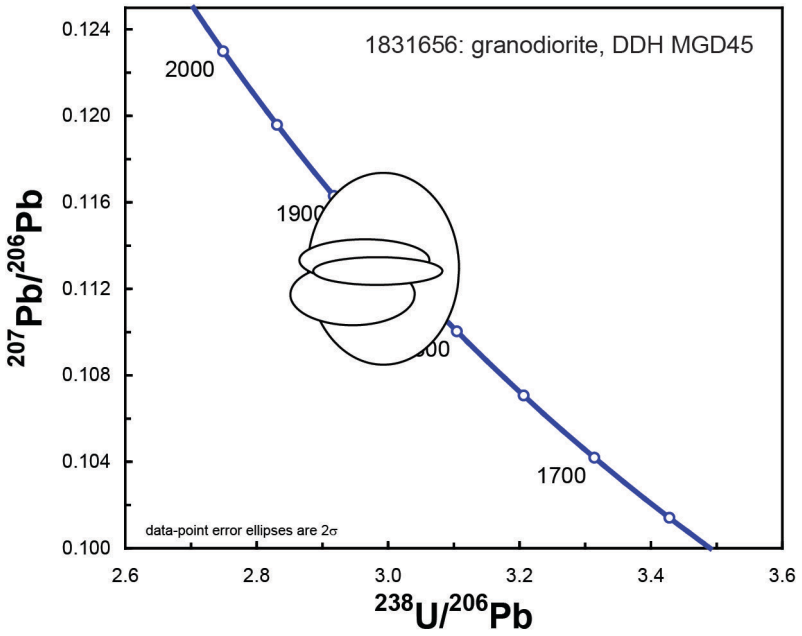

Figure 12. Concordia diagram for sample 1831656.

1848980, CLASTIC SEDIMENT, DDH MGD44, CHIANTI PROSPECT

Sample information

Sample Number:	1848980		
Collector:	A Reid		
Stratigraphic Unit:	unassigned		
Location GDA94:	714372	714372	Zone 53
Location Lat-Long:	-31.267661	137.251575	
250K map sheet	SH5316 TORRENS		
100K map sheet	6335 ARCOONA		
Location:	DDH MGD44, 425.60–426.00 m		
Mount:	1848980-Mount		
Date analysed:	18th May 2011		
Machine:	New Wave LA-ICPMS Adelaide Microscopy		
Concurrent Standard data	Plešovice standard: 339.6 ± 6.5 Ma (n= 3, MSWD = 1.18, probability = 0.31		
Interpreted age:	n/a		
Age type:			
Age calculation method			

Background

The stratigraphy of the MDG 44 drillhole is the most complicated in the series of MGD holes from Chianti (Fig. 13). There is evidence for a conglomerate at the base of the hole, above a typical granite similar to that dated from sample 1831656, and thus likely Donington Suite. The stratigraphic position of this conglomerate is uncertain and it may indicate that the large sections of Donington Suite granite that are located above this are large boulders within a broader sedimentary sequence that includes the laminated sediment and conglomerate between 451.6 – 394.0m (Fig. 13). A possible alternative interpretation is that this conglomerate represents fill of a narrow crack within the basement granites that was present during deposition of the sedimentary rocks preserved between 451.6 – 394.0m.

Sample 1848980 is a clastic sediment (Fig. 14) taken in order to investigate the detrital zircon population within sediments.

Petrography

This sample is a fine grained sediment composed almost entirely of angular to subangular quartz (70%); minor plagioclase and microcline were also observed within the sediment (<5%). Detrital muscovite flakes are present as elongate crystals up to 200 μm in length (<5%; Fig. 15). These clasts are enveloped within a very fine-grained sericite-rich matrix that comprises the remainder of the rock (20%). At the cm scale the rock can be seen to possess laminations of hematite-rich or hematite-poor zones, and this zonation is likely due to subsequent alteration that overprints the laminated sediment. At one end of the thin section there is a ~1 cm wide layer, orange in colour that is very fine grained, comprised of microcrystalline material and sericite-rich alteration. Some acicular voids within this layer suggest it may be tuffaceous and the texture is suggestive of a volcanic-derived layer or layers.

The quartz within the fine-grained sediment consists of single crystals, with very few examples of undulose extinction, suggesting the source of these quartz either has undergone very little deformation and is possibly granitic, or is a high-grade metamorphic rock with extensively recrystallised quartz.

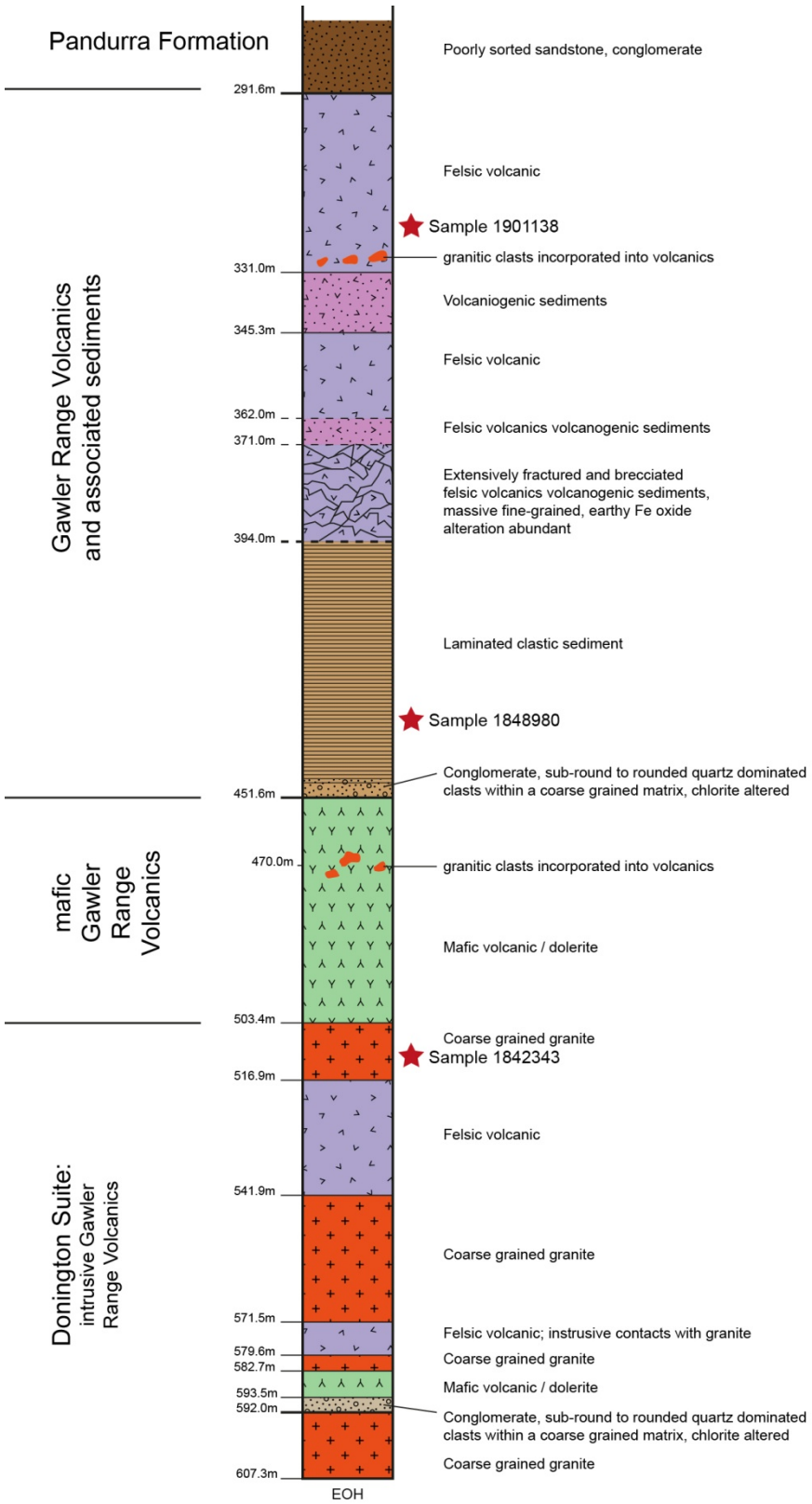

Figure 13. Schematic log of drillhole MGD 44.

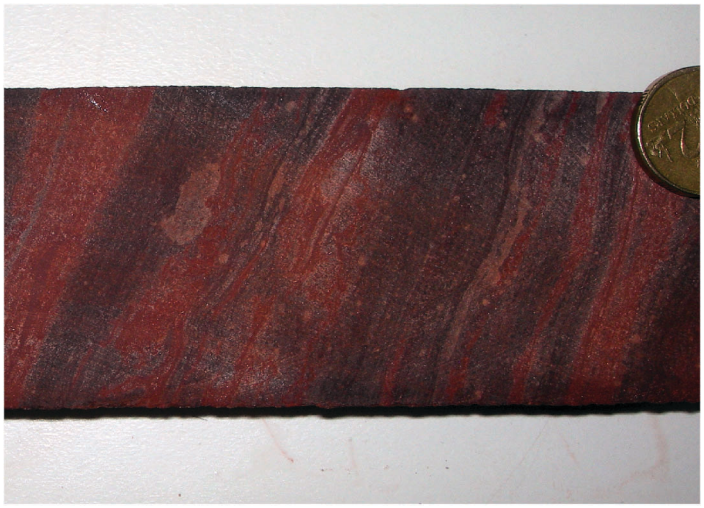

Figure 14. Photograph of laminated, hematite-altered clastic sediment sample 1848980.

Zircon characteristics

Very few zircons were recovered from this sample. The zircons are very poor quality, being extensively fractured and brown in colour. Under CL, the zircons show uniform black response, indicative of high U contents. Under backscatter electron imagery, some zonation is apparent within the zircons (Fig. 16); this appears to be regular in most examples and is likely to be magmatic in origin.

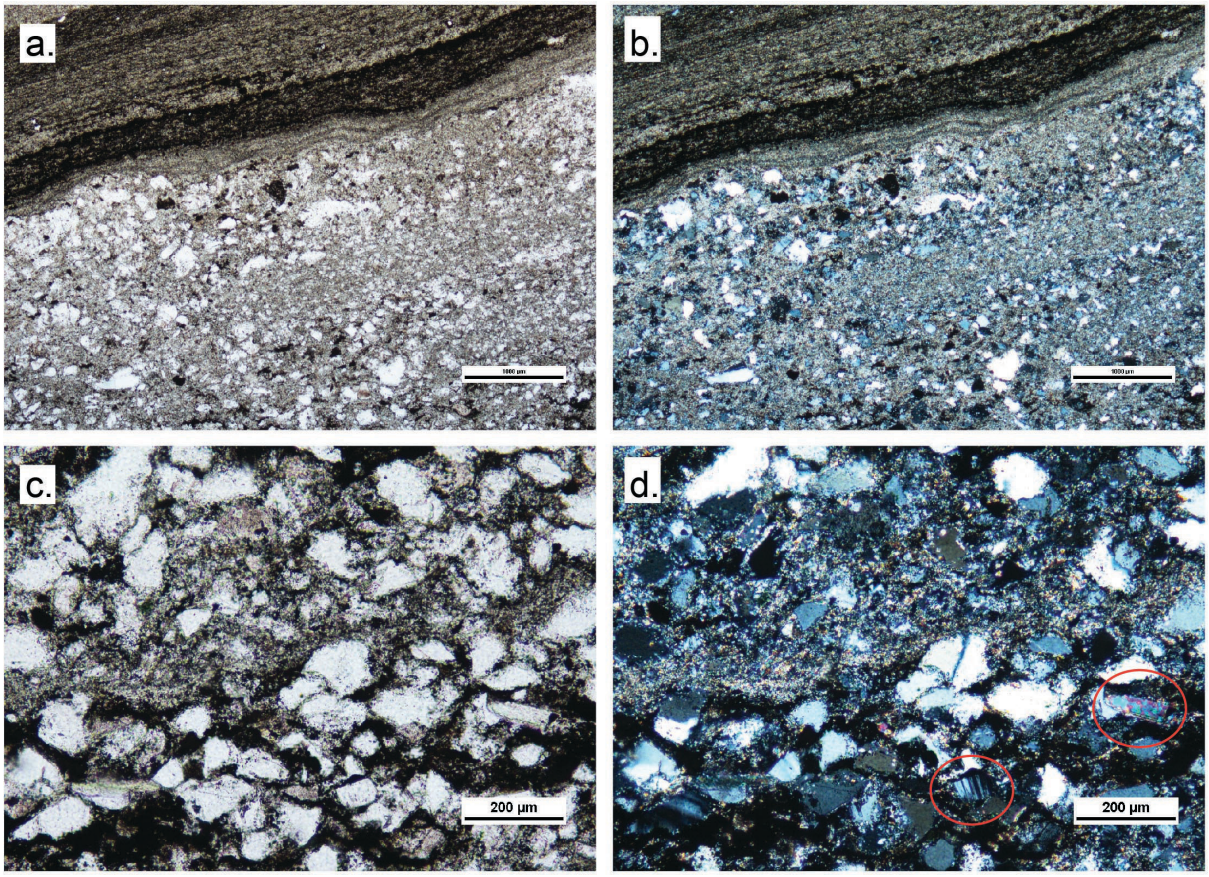

Figure 15. Photomicrographs of sample 1848980. a. Top portion of samples shows the laminated, tuffaceous sediment. Lower portion is the clastic sediment. Transmitted plain polarised light. **b.** Cross polars. **c.** Detail of the clastic sediment, showing the hematite alteration . Transmitted plain polarised light. **d.** Cross polars image of same field of view as in c.; muscovite and feldspar detrital grains circled.

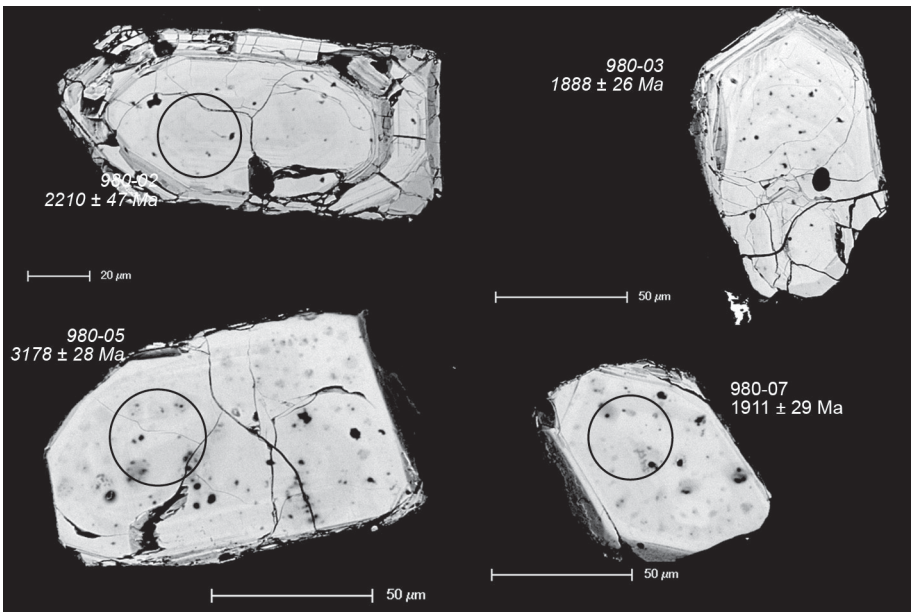

Figure 16. Representative backscatter electron microscopy image of zircons from sample 1848980.

Geochronological results

Only ten zircons were analysed from this sample, due to their poor quality (Table 5). Four of these analyses are <10% discordant (Fig. 17). The ages of these near concordant zircons range from c. 1943 Ma to c. 1903 Ma. This is an interesting result, since there is only one rock that has been dated in South Australia that has an age close to this; an orthogneiss from the GOMA DDH 1, located on the Karari Fault zone between the Coober Pedy and Mabel Creek domains, which was emplaced at 1919 ± 9 Ma (Jagodzinski and Reid, 2010). The remaining data from sample 1848980 span from c. 3180 Ma to c. 1844 Ma (Table 5). However, since these data are considerably discordant the geological significance of the ages is uncertain.

Geochronological interpretation

The geological significance of the very small data set is uncertain; however, this sediment may record input from c. 1920 Ma source region. No statistically significant 'maximum depositional age' can be calculated from the limited data. No c. 1590 Ma zircons were found in the small number of zircons analysed. Follow up analyses of zircons from this sediment is required, preferably using SHRIMP, to confirm if c. 1920 Ma zircons are represented in the detrital population; or if these zircons are affected by non-radiogenic Pb.

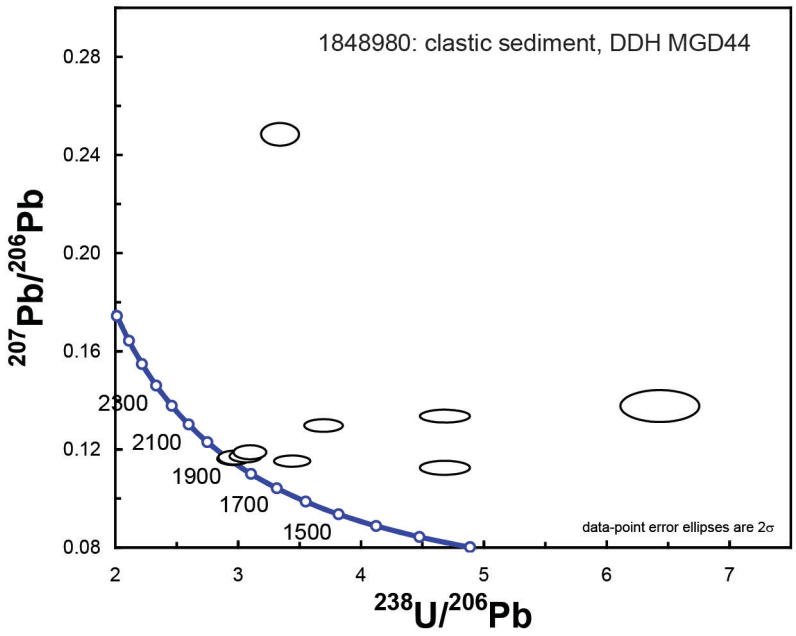

Figure 17. Concordia diagram for sample 1848980.

Table 5. Summary of LA-ICPMS data for sample 1848980.

Analysis	Isotopic ratio						Age				
	Pb^{207}/Pb^{206}	1σ	Pb^{206}/U^{238}	1σ	Pb^{207}/U^{235}	1σ	Pb^{207}/Pb^{206}	1σ	Pb^{206}/U^{238}	1σ	% Disc.
980-06	0.1165	0.0018	0.3384	0.0061	5.433	0.111	1903	28	1879	30	1
980-07	0.1170	0.0019	0.3370	0.0060	5.435	0.111	1911	29	1872	29	2
980-09	0.1175	0.0017	0.3274	0.0058	5.303	0.105	1919	26	1826	28	5
980-10	0.1191	0.0018	0.3237	0.0058	5.312	0.108	1943	27	1808	28	7
980-03	0.1155	0.0017	0.2911	0.0052	4.635	0.090	1888	26	1647	26	13
980-01	0.1300	0.0020	0.2709	0.0047	4.854	0.092	2098	26	1546	24	26
980-04	0.1127	0.0019	0.2139	0.0038	3.322	0.068	1844	30	1249	20	32
980-08	0.1340	0.0019	0.2138	0.0038	3.944	0.077	2150	25	1249	20	42
980-05	0.2489	0.0044	0.3000	0.0057	10.285	0.209	3178	28	1691	28	47
980-02	0.1386	0.0038	0.1556	0.0032	2.957	0.083	2210	47	932	18	58

1842343, GRANITE, DDH MGD44, CHIANTI PROSPECT

Sample information

Sample Number:	1842343		
Collector:	A Reid		
Stratigraphic Unit:	Donington Suite		
Location GDA94:	714372	6538547	Zone 53
Location Lat-Long:	-31.267661	137.251575	
250K map sheet	SH5316 TORRENS		
100K map sheet	6335 ARCOONA		
Location:	DDH MGD44, 511.30–511.70 m		
Mount:	1842343 - Mount		
Date analysed:	13th October 2011		
Machine:	New Wave LA-ICPMS Adelaide Microscopy		
Concurrent Standard data	Plešovice standard: 339.6 ± 6.5 Ma (n= 3, MSWD = 1.18, probability = 0.31		
Interpreted age:	1858 ± 22 Ma		
Age type:	Magmatic crystallisation		
Age calculation method	Weighted mean $^{207}Pb/^{206}Pb$ age		

Background

This sample is an altered granite that is apparently intruded by both altered dolerite and dacite within drill hole 1842343 (Fig. 13). The sample was taken in order to determine if this granite is intrusive into the sediment or whether it may be potentially a large boulder, associated with the conglomerate towards the base of the drill hole (Fig. 13).

Petrography

This sample is a tonalite being rich in plagioclase (45%), with subordinate quartz (25%) and altered biotite (25%), and minor opaque species, possibly magnetite (<1%; Fig. 18). The sample also contains accessory zircon and apatite and along with alteration-related rutile and chlorite (<2%). Both plagioclase and biotite are extensively altered. The plagioclase is coarse grained and almost entirely replaced by fine sericite. Where the lamellar twinning is preserved, the composition indicated by the extinction angle of the twins is approximately $An_{40.}$ A number of the plagioclase crystals have sericite clots formed at ~25° to the orientation of the twins, suggesting the sericite is replacing former inclusions of K-feldspar, present as microperthite in the precursor plagioclase. The quartz is medium-grained. The triple junctions between quartz grains and the only minor undulose extinction present in some grains suggests the rock has undergone very little strain. Biotite occurs interstitially to the leucocratic phases in the rock and has a very light green plieochroism and is extensively altered with dark brown and light green patches, possibly related to clays, chlorite and or sericite. Needles of rutile intergrown with the biotite are common.

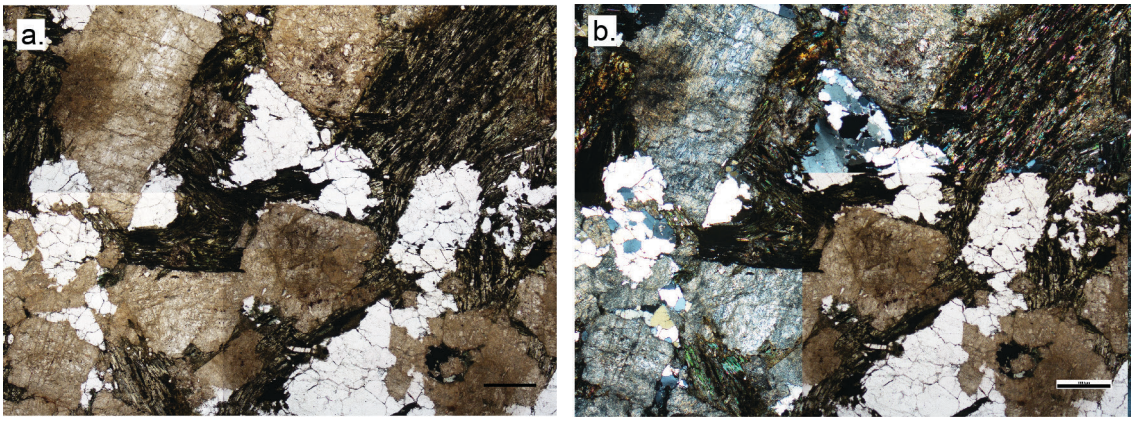

Figure 18. Photomicrograph of sample 1842343. Bar at lower right is 1 mm. a. Plain polarised light. **b.** Cross polars.

Zircon characteristics

The zircons from this sample are extensively fractured and brown in colour (Fig. 19). Under CL, the zircons are clearly euhedral grains with moderate length to width ratios. Oscillatory zonation is evident in most examples, with some showing evidence for central core regions which are dominated by a very high U, dark phase. The zircons are magmatic in origin.

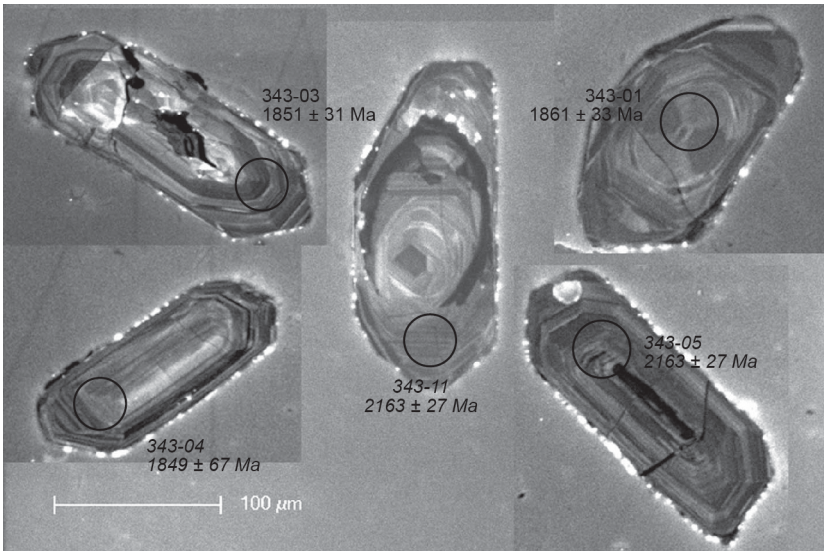

Figure 19. Representative CL image of zircons from sample 1842343. Circles indicate analytical site. Italics in the numbers indicates data is >10% discordant. Plain light image not available.

Geochronological results

Approximately half of the nineteen zircons analysed from this sample produced discordant to strongly discordant data (Table 6). The discordant zircon analyses plot towards non-radiogenic compositions on a Tera-Wasserburg diagram (Fig. 20), indicating the presence of non-radiogenic Pb. The near concordant to concordant analyses, however, cluster at c. 1855 Ma, and a weighted mean $^{207}Pb/^{206}Pb$ age calculated from 8 of these data is 1858 ± 22 Ma (MSWD = 0.021, probability = 1.0).

Geochronological interpretation

Given the simple igneous nature of the zircons from this sample, the weighted mean $^{207}Pb/^{206}Pb$ age of 1858 ± 22 Ma is interpreted to be the best estimate of timing of crystallisation of the granite. The basal granite within DDH MGD44 is very similar to other granites dated in this study and is correlated with these c. 1855 Ma Donington Suite granites. Sample 1842343 is also part of the Donington Suite.

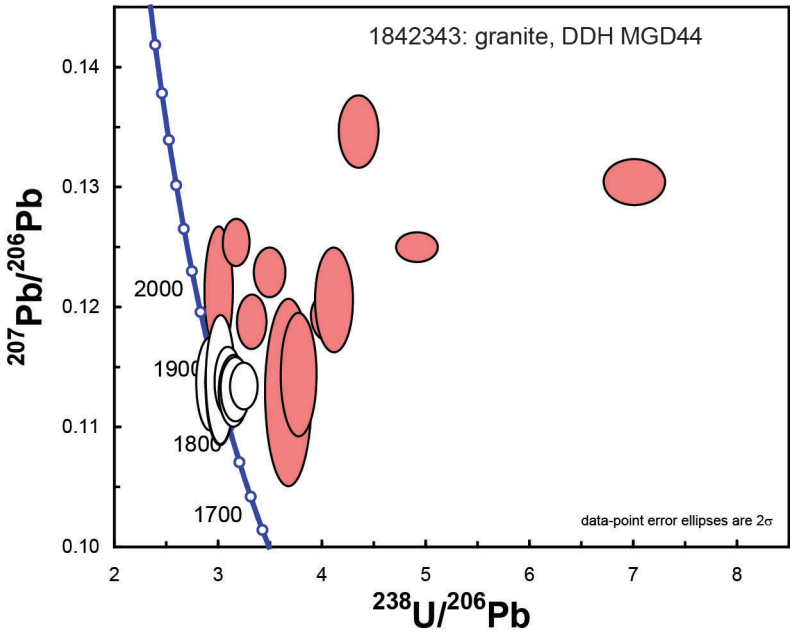

Figure 20. Concordia diagram for sample 1842343.

Table 6. Summary of LA-ICPMS data for sample 1842343.

Analysis	Isotopic ratio						Age				
	Pb^{207}/Pb^{206}	1σ	Pb^{206}/U^{238}	1σ	Pb^{207}/U^{235}	1σ	Pb^{207}/Pb^{206}	1σ	Pb^{206}/U^{238}	1σ	% Disc.
Analyses used in age calculation; near concordant data											
343-14	0.1140	0.0023	0.3418	0.0065	5.357	0.127	1864	35	1896	31	-2
343-09	0.1133	0.0027	0.3317	0.0062	5.185	0.132	1854	43	1847	30	0
343-01	0.1138	0.0021	0.3327	0.0063	5.223	0.114	1861	33	1851	30	1
343-02	0.1139	0.0030	0.3316	0.0064	5.212	0.141	1863	47	1846	31	1
343-16	0.1139	0.0019	0.3237	0.0056	5.080	0.102	1862	29	1808	27	3
343-13	0.1137	0.0019	0.3184	0.0060	4.964	0.107	1859	30	1782	29	4
343-03	0.1132	0.0019	0.3162	0.0059	4.934	0.104	1851	31	1771	29	4
343-15	0.1213	0.0030	0.3331	0.0062	5.579	0.144	1975	43	1853	30	6
343-08	0.1135	0.0015	0.3084	0.0052	4.825	0.088	1855	24	1733	26	7
Discordant analyses											
343-12	0.1190	0.0016	0.3015	0.0053	4.940	0.095	1941	24	1699	26	12
343-10	0.1255	0.0016	0.3155	0.0053	5.458	0.099	2036	22	1768	26	13
343-04	0.1130	0.0043	0.2723	0.0068	4.240	0.160	1849	67	1553	34	16
343-06	0.1140	0.0029	0.2653	0.0050	4.185	0.110	1864	46	1517	25	19
343-17	0.1230	0.0016	0.2865	0.0050	4.857	0.091	2000	23	1624	25	19
343-07	0.1193	0.0016	0.2464	0.0042	4.051	0.075	1945	24	1420	22	27
343-18	0.1206	0.0026	0.2431	0.0044	4.044	0.095	1965	37	1403	23	29
343-11	0.1349	0.0021	0.2301	0.0041	4.274	0.086	2163	27	1335	22	38
343-05	0.1250	0.0015	0.2037	0.0034	3.511	0.060	2029	20	1195	18	41
343-19	0.1306	0.0016	0.1427	0.0025	2.568	0.047	2106	21	860	14	59

SHRIMP GEOCHRONOLOGY RESULTS

1901138, FELSIC VOLCANIC, DDH MGD44, CHIANTI PROSPECT

Sample information

Sample Number:	1901138		
Collector:	A Fabris		
Stratigraphic Unit:	Gawler Range Volcanics		
Location GDA94:	714372	6538547	Zone 53
Location Lat-Long:	-31.267661	137.251575	
250K map sheet	SH5316 TORRENS		
100K map sheet	6335 ARCOONA		
Location:	DDH MGD44, 326.15–327.90 m		
Mount:	Mount AR-28		
Date analysed:	10th June 2012		
Machine:	SHRIMP A, Curtin University		
Concurrent Standard data	See Appendix		
Interpreted age:	1591 ± 10 Ma		
Age type:	Magmatic crystallisation		
Age calculation method	Weighted mean $^{207}Pb/^{206}Pb$ age		
Interpreted age:	c. 1870 Ma		
Age type:	n/a		
Age calculation method	inheritance		

Background

The present sample is of the dacitic microgranite or subvolcanic rock that is intercalated with a section of medium grained sediment, which includes possible tuffaceous horizons. Several of these dacite/microgranite intervals occur within this drillhole. Sample 1901138 is a fine-grained massive cream rock that is moderately hard (Fig. 21a). It is cut by at least two generations of fractures relating to near-surface oxidation processes: early thin discontinuous fractures are closely spaced and define a set filled by black mineral; these are overprinted by thicker fractures filled by hematite (Fig. 21b). This zone of sub-volcanic rock also shows an abundance of xenolithic clasts, particularly in the lower portion of the interval, around 331m (Fig. 21c) and in places the rock appears to be breciated, with the volcanic material enclosing clasts of fractured granite, and zones of intense hematite alteration (Fig. 21d).

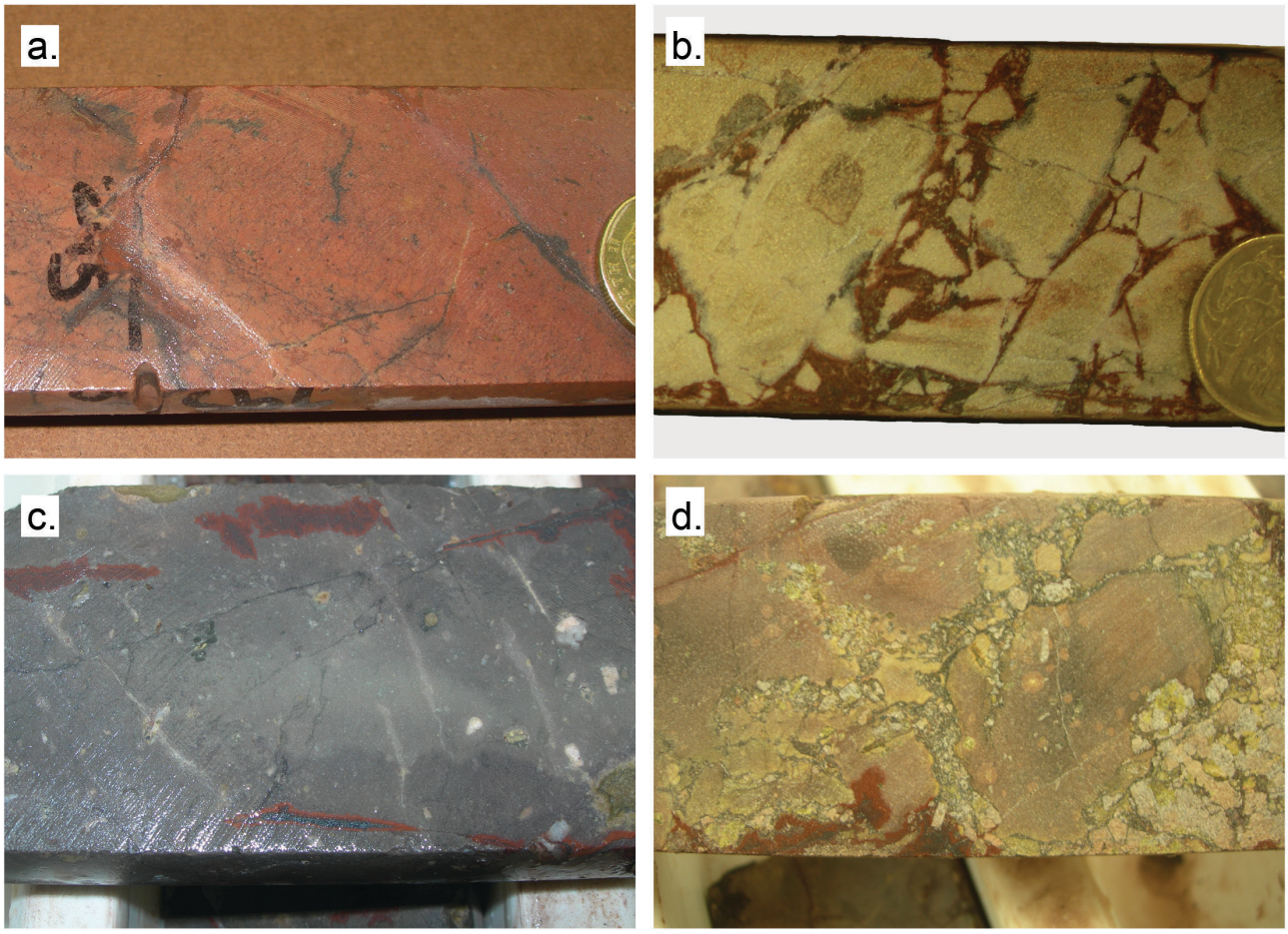

Figure 21. Features of the felsic volcanic/microgranite interval within drill hole MGD 44. a. Pink coloured fine-grained felsic rock at c. 295m, very close to where sample 1901138 was taken. **b.** One section of this interval of felsic volcanic showing hematite-filled fractures from around 345m. **c.** Detail showing hematite stained fractures plus clasts of K-feldspar+quartz representing xenoliths of granitic material within this felsic volcanic, at around 340m. **d.** Zone of breccia near 329m.

Petrography

The following description is from Mason Geoscience Petrology Report 2012_04_MG3830.

A visual estimate of the modal mineral abundances gives the following:

Mineral	Vol	%	Origin
Quartz	35	Igneous	1
Sericite	59	Alteration	2
?Zircon	Tr	Igneous	1
Rutile	Tr	Alteration	2
Quartz	Tr	Veinlet fillings	2
Hematite	5	Weathering	3 (fracture seals 3)

In thin section, this sample displays a poorly-preserved massive crystalline texture of probable igneous origin, severely modified by thin veining, pervasive alteration, and subsequent oxidation (Fig. 22. Quartz is moderately abundant, forming small anhedral grains ~100 μ m in size. They are uniformly distributed through the rock, and their angular shapes suggest they formed as interstitial primary igneous grains. Sericite is abundant, forming tiny flecks which tend to be concentrated in aggregates distributed throughout the rock. In places, small prismatic crystal shapes are preserved: these may have been ?plagioclase, an interpretation supported by the observation that their shapes are enhanced where they are enclosed by adjacent interstitial quartz.

Rutile occurs in trace amount as tiny granules in the sericite aggregates. Thin quartz veinlets cut the rock, and contain anhedral clear quartz grains. Hematite occurs in significant amount, and different sites are observed:

1. Some hematite forms fine-grained dense replacements of precursor angular grains in the quartz-bearing veinlets. The identity of the precursor vein-forming phase remains unknown.
2. Some hematite forms a more diffuse margin away from the veinlets, encroaching into host rock.

Possible ?zircon occurs as rare small stumpy terminated prisms ~15 µm in size. One crystal has been observed where it formed as a euhedral crystal epitaxial to a (now rutile-altered) Fe-Ti oxide crystal. Very thin tortuous microfractures (black in hand sample) are observed in the thin section, but are too fine-grained for positive mineral identification.

This sample is interpreted to have initially formed as a uniformly fine-grained felsic igneous rock, possibly a microgranitoid. Primary quartz formed in moderate amount as even-sized small angular interstitial grains.

Most other minerals, except trace small ?zircon crystals, have been destroyed in response to an alteration event when thin fractures were sealed by quartz + unknown others, and host rock was replaced by abundant sericite + trace rutile. Subsequent weathering generated new goethite, mainly concentrated along the precursor thin veinlets.

Note that trace zircon may be present. The crystals are too small for observation under transmitted light, where they are hidden within fine-grained sericite because they are smaller than the thickness of the section. However, even small zircons can be found under plane reflected light, where they are cleanly intersected by the section surface and their optical characteristics aid recognition: clean appearance, paler grey than quartz, some internal reflections, no cleavage.

Zircon characteristics

The zircons recovered from this sample are heterogeneous (Fig. 23). There is a population of coarse dark coloured grains that are anhedral to subhedral in morphology. There are also numerous grains that are subhedral and clear in colour. The CL response for almost all of the grains is uniformly dark, indicative of relatively high U contents.

Geochronological results

Thirteen analyses were made on thirteen zircons from this sample (Table 7). Six of these are near concordant and cluster at $^{207}Pb/^{206}Pb$ age of c. 1590 Ma (Fig. 24). These analyses derive mostly from the larger zircons within the mineral separate and are probably the grains that record the magmatic crystallisation age of the sample. A weighted mean $^{207}Pb/^{206}Pb$ age calculated from these zircons is 1591 ± 10 Ma (n = 6, MSWD = 0.42, probability = 0.83).

The remaining 7 are have ages that range from c. 1641 Ma to c. 1898 Ma (Table. 7). These grains may be inherited zircon within the magmatic rock. The near concordant analyses at c. 1870 Ma likely reflect inheritance from the local host rock (Donington Suite). The significance of the remaining c. 1713–1641 Ma grains is uncertain.

Geochronological interpretation

Given the simple igneous nature of the zircons from this sample, the weighted mean $^{207}Pb/^{206}Pb$ age of 1591 ± 10 Ma is interpreted to be the best estimate for the timing of emplacement of this fine grained felsic igneous rock. The presence of inherited zircons is consistent with the observed xenoliths of granite preserved within portions of this fine-grained felsic rock.

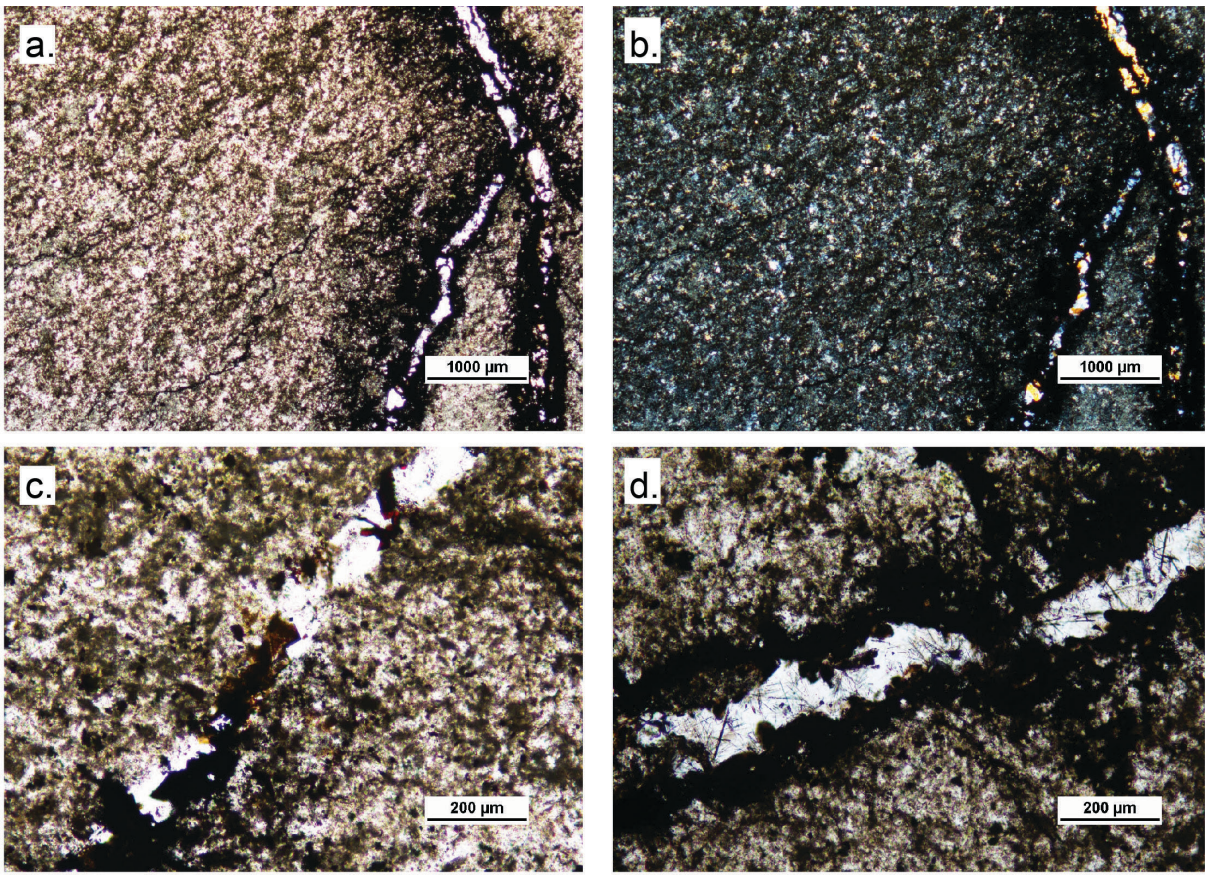

Figure 22. Photomicrograph of sample 1901138. a. Plain polarised light. **b.** Cross polars. **c.** Detail of one of the quartz veinlets with hematite. **d.** Detail of one quartz veinlet with rutile needles intergrown with the quartz.

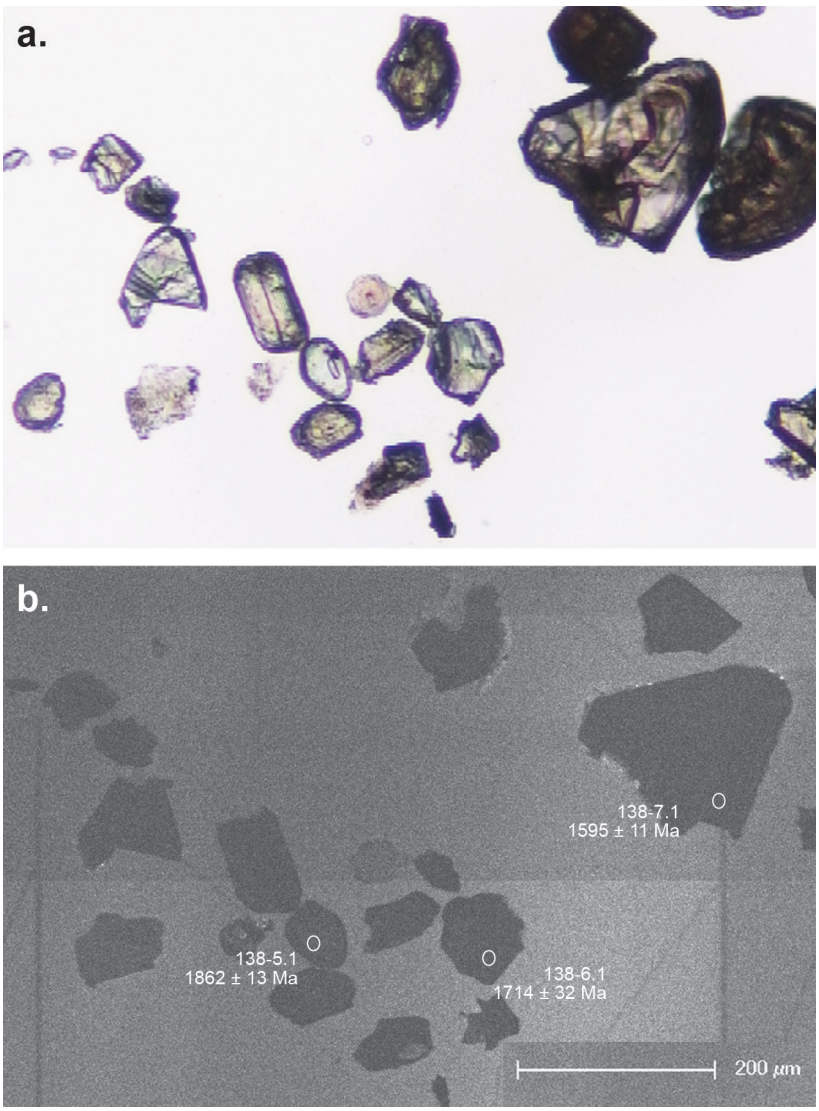

Figure 23. Representative CL image of zircons from sample 1842343. a. Plain light image. **b.** CL image. Circles indicate SHRIMP analytical sites.

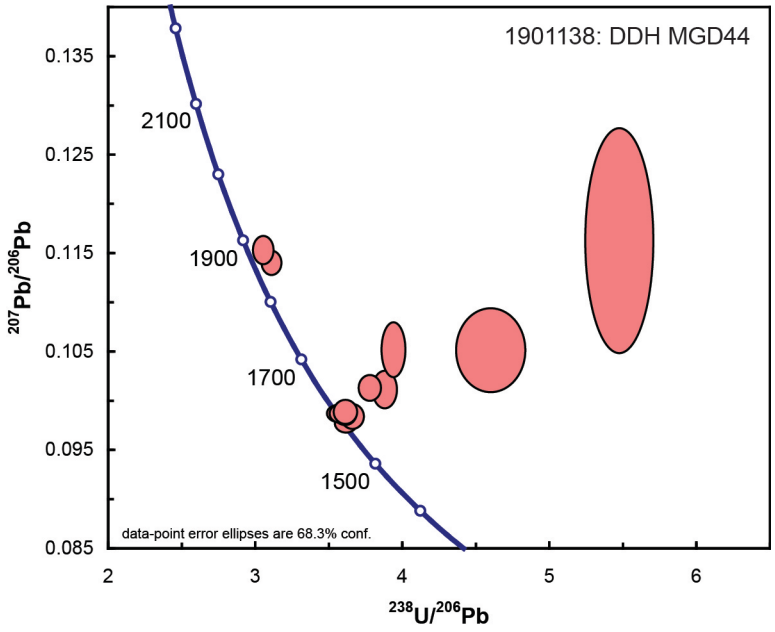

Figure 24. Concordia diagram for sample 1901138.

Table 7. Summary of SHRIMP U-Pb zircon analyses from sample 1901138.

Spot	ppm U	ppm Th	$^{232}Th/^{238}U$	$^{206}Pb^*/^{238}U$	±%	$^{207}Pb^*/^{235}U$	±%	$^{207}Pb^*/^{206}Pb^*$	±%	$^{207}Pb^*/^{206}Pb^*$	±	% Disc
magmatic population												
138-10.1	260	267	1.06	0.2773	1.39	3.726	1.531	0.1018	1.67	1576	12	0
138-3.1	181	218	1.25	0.2740	1.46	3.710	1.691	0.1066	1.89	1590	16	2
138-2.1	169	180	1.10	0.2779	1.45	3.773	1.659	0.1013	1.62	1595	15	1
138-7.1	314	391	1.29	0.2820	1.35	3.829	1.468	0.1018	1.73	1595	11	0
138-13.1	241	199	0.85	0.2805	1.38	3.808	1.525	0.1004	1.10	1595	12	0
138-4.1	149	151	1.05	0.2776	1.49	3.775	1.709	0.1011	1.59	1598	16	1
discordant analyses: inheritance												
138-12.1	255	395	1.60	0.2584	1.42	3.596	1.900	0.1024	6.95	1641	23	11
138-1.1	412	348	0.87	0.2655	1.35	3.701	1.594	0.0980	1.31	1644	16	9
138-8.1	147	212	1.49	0.2177	3.40	3.149	4.337	0.0772	6.07	1713	50	29
138-6.1	340	290	0.88	0.2544	1.35	3.682	2.221	0.0938	2.15	1714	32	16
138-11.1	159	244	1.59	0.1826	2.81	2.926	7.123	0.1758	10.29	1898	118	47
138-5.1	144	75	0.53	0.3230	1.46	5.073	1.636	0.1137	0.93	1862	13	4
138-9.1	125	69	0.57	0.3289	1.53	5.224	1.735	0.1158	0.99	1883	15	3

SUMMARY

The data presented here shows that the predominant host rock lithology within the Chianti prospect is the Donington Suite. The Donington Suite has been confirmed by dating of zircons from granitic samples from drillholes MGD 44, 45 and 46.

There is immature sediment intersected in drill hole MGD 44 and this sediment contains zircons with ages that are poorly constrained, but which appear to record input from a c. 1920 Ma source region. It is noted that no c. 1590 Ma zircons were found in the small number of zircons analysed from the sediment sample, and that the zircons suffered from high non-radiogenic Pb combined with Pb loss, that make the significance of the ages derived from them questionable.

The prospect appears to be intruded by a series of c. 1590 Ma Gawler Range Volcanics-related fine grained felsic rocks. Mafic intrusives are also present, which are potentially also associated with the Gawler Range Volcanics, however, geochemical comparison is required to confirm this.

The c. 1855 Ma granitic suite that hosts the weak mineralisation present within drill hole MGD34 has been extensively altered. The timing of this alteration remains unconstrained but is most likely associated with the regional c. 1590 Ma alteration and mineralisation event within the Olympic Cu-Au Province. Further work on the dating of this prospect could focus on the sedimentary rocks to determine the provenance with more certainty, and on determining the timing and geochemistry of the mafic magmatism present as intrusive dolerites within a number of the drill holes.

ACKNOWLEDGEMENTS

E Jagodzinski processed the SHRIMP data for sample 1901138 and reviewed the text.

APPENDIX 1

SHRIMP STANDARD BEHAVIOR

Nine analyses of Temora during the analysis of sample **1901138** have a $^{206}Pb^*/^{238}U$ calibration uncertainty of 0.48%, and an external spot-to-spot (reproducibility) uncertainty of 0% (1σ). A more realistic value of 1% is applied to the data processing. The value of 2 is used for the calibration slope. The $^{207}Pb/^{206}Pb$ age of Temora is 437 ± 66 Ma (weighted mean) or 456 ± 81 Ma (Tukey's biweight) and there is no suggestion of overcounts on the Pb peaks. Five analyses of OG1 yield a weighted mean $^{207}Pb/^{206}Pb$ age of 3464.4 ± 4.7 Ma (MSWD = 0.7, probability of fit = 0.59). No correction for IMF has been applied to this session.

REFERENCES

Belousova, E., Griffin, W.L., Shee, S.R., Jackson, S.E., O'Reilly, S.Y., 2001. Two age populations of zircons from the Timber Creek kimberlites, Northern Territory, as determined by laser-ablation ICPMS analysis. Australian Journal of Earth Sciences 48, 757-765.

Black, L.P., Kamo, S.L., Williams, I.S., Mundil, R., Davis, D.W., Korsch, R.J., Foudoulis, C., 2003. The application of SHRIMP to Phanerozoic geochronology; a critical appraisal of four zircon standards. Chemical Geology 200, 171-188.

Griffin, W.L., Powell, W.J., Pearson, N.J., O'Reilly, S.Y., 2008. GLITTER: data reduction software for laser ablation ICP-MS, Laser Ablation-ICP-MS in the Earth Sciences. Mineralogical Association of Canada Short Course Series vol. 40, pp. 204-207.

Hayward, N., Skirrow, R., 2010. Geodynamic setting and controls on iron oxide Cu-Au (±U) ore in the Gawler Craton, South Australia, in: Porter, T.M. (Ed.), Hydrothermal iron oxide copper-gold and related deposits: A global perspective, volume 3, Advances in the understanding of IOCG deposits. PGC Publishing, Adelaide, pp. 105-131.

Jackson, S.E., Pearson, N.J., Griffin, W.L., Belousova, E.A., 2004. The application of laser ablation-inductively coupled plasma-mass spectrometry to in situ U-Pb zircon geochronology. Chemical Geology 211, 47-69.

Jaffey, A.H., Flynn, K.F., Glendenin, L.E., Bentley, W.C., Essling, A.M., 1971. Precision Measurement of Half-Lives and Specific Activities of 235U and 238U. Physical Reviews C 4, 1889-1906.

Jagodzinski, E., Reid, A.J., 2010. New zircon and monazite geochronology using SHRIMP and LA-ICPMS, from recent GOMA drilling, on samples from the northern Gawler Craton, in: Korsch, R.J., Kositcin, N. (Eds.), GOMA (Gawler Craton-Officer Basin-Musgrave Province-Amadeus Basin) Seismic and MT Workshop 2010. Geoscience Australia, Record, 2010/39, pp. 108-117.

Jagodzinski, E.A., 2005. Compilation of SHRIMP U-Pb geochronological data, Olympic Domain, Gawler Craton, South Australia, 2001-2003. Geoscience Australia Record 2005/20, 211.

Ludwig, K.R., 2003. Isoplot 3.00 - a geochronological toolkit for Microsoft Excel. Berkeley Geochronology Center Special Publication No. 4.

Ludwig, K.R., 2009. SQUID 2.50: A user's manual. Berkeley Geochronology Center Special Publication No. 5., Berkeley California, USA.

McPhie, J., Kamenetsky, V.S., Chambefort, I., Ehrig, K., Green, N., 2011. Origin of the supergiant Olympic Dam Cu-U-Au-Ag deposit, South Australia: Was a sedimentary basin involved? Geology 39, 795-798.

Paterson, H.L., 2007. Unlocking South Australia's Mineral and Energy Potential - A Plan for Accelerating Exploration. Theme 2 (drilling partnerships with PIRSA and industry) : Year 4 partnership no. 65, Chianti mineral prospect. Project completion dataset. South Australia. Department of Primary Industries and Resources. Open file Envelope, 11557. Unpublished.

Payne, J., Barovich, K., Hand, M., 2006. Provenance of metasedimentary rocks in the northern Gawler Craton, Australia: Implications for Palaeoproterozoic reconstructions. Precambrian Research 148, 275-291.

Reid, A., Payne, J., Wade, B., 2006. A new geochronological capability for South Australia: U-Pb zircon dating via LA-ICPMS. MESA Journal 42, 27-37.

Skirrow, R.G., Bastrakov, E., Barovich, K., Fraser, G., Fanning, C.M., Creaser, R., Davidson, G., 2007. The Olympic Cu-Au province: timing of hydrothermal activity, sources of metals, and the role of magmatism. Economic Geology 102, 1441-1470.

Sláma, J., Košler, J., Condon, D.J., Crowley, J.L., Axel, G., Hanchar, J.M., Horstwood, M.S.A., Morris, G.A., Nasdala, L., Norberg, N., Schaltegger, U., Schoene, B., Tubrett, M.N., Whitehouse, M.J., 2007. Plešovice zircon - A new natural reference material for U–Pb and Hf isotopic microanalysis. Chemical Geology 249, 1-35.

Stacey, J.S., Kramers, J.D., 1975. Approximation of terrestrial lead isotope evolution by a two-stage model. Earth and Planetary Science Letters 26, 207-221.

Steiger, R.H., Jäger, E., 1977. Subcommission of geochronology: convention on the use of decay constants in geo- and cosmochronology. Earth and Planetary Science Letters 36, 359-362.

Stern, R.A., Bodorkos, S., Kamo, S.L., Hickman, A.H., Corfu, F., 2009. Measurement of SIMS instrumental mass fractionation of Pb isotopes during zircon dating. Geostandards and Geoanalytical Research 33, 145-168.